Kinetics of the Inhibition of Bovine Liver Dihydrofolate Reductase by Tea Catechins: Origin of Slow-Binding Inhibition and pH Studies†

Enma Navarro-Perán,‡ Juan Cabezas-Herrera,§ Alexander N. P. Hiner,‡ Tinatin Sadunishvili,|| Francisco García-Cánovas,‡ and José Neptuno Rodríguez-López*,‡

Grupo de Investigación de Enzimología, Departamento de Bioquímica y Biología Molecular A, Facultad de Biología, Universidad de Murcia, Murcia, Spain, Servicio de Análisis Clínicos, Hospital Universitario Virgen de la Arrixaca, Murcia, Spain, and Biotechnology Department, Durmishidze Institute of Biochemistry and Biotechnology, Tbilisi, Georgia

Received January 27, 2005; Revised Manuscript Received April 6, 2005

ABSTRACT: Dihydrofolate reductase (DHFR) is the subject of intensive investigation since it appears to be the primary target enzyme for "antifolate" drugs, such as methotrexate and trimethoprim. Fluorescence quenching and stopped-flow fluorimetry show that the ester bond-containing tea polyphenols (−)-epigallocatechin gallate (EGCG) and (−)-epicatechin gallate (ECG) are potent and specific inhibitors of DHFR with inhibition constants (K_I) of 120 and 82 nM, respectively. Both tea compounds showed the characteristics of slow-binding inhibitors of bovine liver DHFR. In this work, we have determined a complete kinetic scheme to explain the slow-binding inhibition and the pH effects observed during the inhibition of bovine liver DHFR by these tea polyphenols. Experimental data, based on fluorimetric titrations, and transient phase and steady-state kinetic studies confirm that EGCG and ECG are competitive inhibitors with respect to 7,8-dihydrofolate, which bind preferentially to the free form of the enzyme. The origin of their slow-binding inhibition is proposed to be the formation of a slow dissociation ternary complex by the reaction of NADPH with the enzyme−inhibitor complex. The pH controls both the ionization of critical catalytic residues of the enzyme and the protonation state of the inhibitors. At acidic pH, EGCG and ECG are mainly present as protonated species, whereas near neutrality, they evolve toward deprotonated species due to ionization of the ester-bonded gallate moiety (pK = 7.8). Although DHFR exhibits different affinities for the protonated and deprotonated forms of EGCG and ECG, it appears that the ionization state of Glu-30 in DHFR is critical for its inhibition. The physiological implications of these pH dependencies are also discussed.

Dihydrofolate reductase (DHFR,[1] 5,6,7,8-tetrahydrofolate: $NADP^+$ oxidoreductase, EC 1.5.1.3) catalyzes the reduction of 7,8-dihydrofolate (DHF) to 5,6,7,8-tetrahydrofolate (THF) in the presence of coenzyme NADPH (DHF + NADPH + H^+ → THF + $NADP^+$). This enzyme is necessary for maintaining intracellular pools of THF and its derivatives which are essential cofactors in one-carbon metabolism. Coupled with thymidylate synthase (*1*), it is directly involved in thymidylate (dTMP) production through a de novo pathway. DHFR is therefore pivotal in providing purines and pyrimidine precursors for the biosynthesis of DNA, RNA, and amino acids. In addition, it is the target enzyme (*2*) for antifolate drugs such as the antineoplastic drug methotrexate (MTX) and the antibacterial drug trimethoprim (TMP). Because of its biological and pharmacological importance, DHFR has been the subject of extensive structural and kinetic studies (*3*−*6*).

Recent studies have presented data that show a variety of biological activities of tea catechins, compounds which constitute ∼15% (dry weight) of green tea (*7*, *8*). Green tea catechins include (−)-epigallocatechin gallate (EGCG), (−)-epigallocatechin (EGC), (−)-epicatechin gallate (ECG), and (−)-epicatechin (EC). EGCG is the most abundant (one 240 mL cup of brewed tea contains up to 200 mg of EGCG), and many health benefits, including antioxidant, antibiotic, and antiviral activities, have been attributed to this compound (*9*−*11*). Some authors consider EGCG alone to be the active anticancer component, while others suggest that other tea constituents also have antiproliferative or anticarcinogenic properties (*12*). Green tea extracts have been shown in vitro to stimulate apoptosis of various cancer cell lines, including prostate, lymphoma, colon, and lung (*7*, *12*−*14*). Moreover, EGCG was reported to inhibit tumor invasion and angiogenesis, processes that are essential for tumor growth and metastasis (*12*). Despite great efforts during the past two

† This work was supported in part by a grant from the EU INTAS Program (Project INTAS00-0727) to T.S., F.G.-C., and J.N.R.-L. and from the Fondo de Investigación Sanitaria (FIS) (Projects 01/3025 and 02/1567) to J.C.-H. E.N.-P. is supported by a fellowship from the Ministerio de Educación y Ciencia, Spain.

* To whom correspondence should be addressed: Grupo de Investigación de Enzimología, Departamento de Bioquímica y Biología Molecular A, Facultad de Biología, Universidad de Murcia, E-30100 Espinardo, Murcia, Spain. Telephone: +34-968-398284. Fax: +34-968-364147. E-mail: neptuno@um.es.

‡ Universidad de Murcia.

§ Hospital Universitario Virgen de la Arrixaca.

|| Durmishidze Institute of Biochemistry and Biotechnology.

[1] Abbreviations: EGCG, (−)-epigallocatechin gallate; EGC, (−)-epigallocatechin; ECG, (−)-epicatechin gallate; EC, (−)-epicatechin; DHFR, dihydrofolate reductase; DHF, 7,8-dihydrofolate; THF, 5,6,7,8-tetrahydrofolate; MTX, methotrexate; TMP, trimethoprim; TMQ, trimetrexate.

10.1021/bi050160t CCC: $30.25
Published on Web 04/30/2005

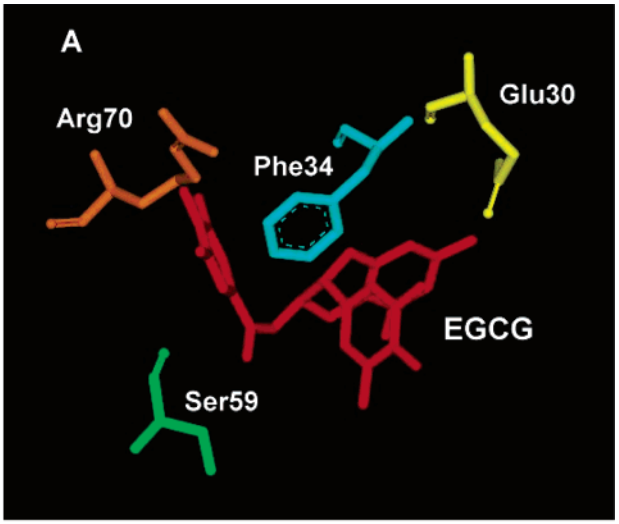

FIGURE 1: (A) Schematic view of EGCG modeled into the folate-binding site of human DHFR. (B) Sequence alignment of bovine and human DHFRs.

decades to understand the anticarcinogenic activity of tea, the exact mechanisms of action are not well defined. Therefore, deciphering the molecular mechanism by which green tea or EGCG imparts its antiproliferative effects could be important and may result in improved opportunities for the treatment of cancer.

On the basis of the observation that classical (MTX) and nonclassical (TMP and TMQ) antifolate compounds possess chemical structures similar to those of some tea polyphenols (*15*), we started to work on the hypothesis that tea catechins could inhibit DHFR activity. Suppression of DNA synthesis by tea catechins could explain many of the observed effects on cancer inhibition by these compounds. Recently, we have shown that ester-bonded gallate catechins isolated from green tea, such as EGCG and ECG, are potent inhibitors of DHFR activity in vitro at concentrations found in the serum and tissues of green tea drinkers (0.1−1.0 μM) (*15*). EGCG exhibited the kinetic characteristics of a slow-binding inhibitor of DHF reduction with bovine liver DHFR but of a classical, reversible, competitive inhibitor with chicken liver DHFR. Structural modeling showed that EGCG can bind to human DHFR in an orientation similar to that observed for a number of structurally characterized DHFR inhibitor complexes (Figure 1A). These results suggested that EGCG could act as an antifolate compound in the same way as MTX and TMP. In this work, we have determined a complete kinetic scheme to explain the slow-binding inhibition and the pH effects observed during the inhibition of bovine liver DHFR by the tea polyphenols, EGCG and ECG. Bovine liver DHFR is a commercially available enzyme which is 87% homologous with human DHFR (Figure 1B), including all those residues believed to be functionally and structurally critical, as identified in the crystal structure of the human enzyme (*3*). This suggests that kinetic analysis of bovine liver DHFR will be a suitable model for future studies of the inhibition of DHFR from other mammalian (including human) sources by EGCG and ECG, and by novel compounds based on their structures (*16*).

EXPERIMENTAL PROCEDURES

Materials. Highly purified tea polyphenols EGCG (>95%), ECG (>98%), EGC (>98%), and EC (>98%) were purchased from Sigma Chemical Co. (Madrid, Spain). Green tea extract was obtained from fresh tea (*Camellia sinensis*) leaves after steam treatment (130 °C) for 2−3 min, to inactivate enzymes. The leaves were then crushed in a CTC (crush, tear, curl) type machine and extracted with hot water (80 °C) at a ratio of 1:10 (w/v). The liquid extract was filtered, concentrated up to 25% dry matter, and spray-dried. Bovine liver DHFR was purchased from Fluka Chemical Co. (Madrid, Spain) and dialyzed exhaustively against distilled water to remove the 1.5 M ammonium sulfate in which it is supplied. The enzyme concentration was determined by MTX titration of the enzyme fluorescence (*17*). DHF was obtained from Aldrich Chemical Co. (Madrid, Spain) and NADPH from Sigma. The concentrations of NADPH and DHF were determined enzymatically at 340 nm using DHFR and a molar absorbance change ($\Delta\epsilon$) for the reaction of 11 800 M^{-1} cm^{-1} at this wavelength (*18*).

Dihydrofolate Reductase Assays and Kinetic Data Analysis. The activity of DHFR was determined at 25 °C by following the decrease in the absorbance of NADPH and DHF at 340 nm in a Perkin-Elmer Lambda-2 spectrophotometer with 1.0 cm light path cuvettes. Experiments were performed in a buffer containing 2-(*N*-morpholino)ethanesulfonic acid (Mes, 0.025 M), sodium acetate (0.025 M), tris(hydroxymethyl)aminomethane (Tris 0.05 M), and NaCl (0.1 M), and the ionic strength remained constant at an optimum value of 0.15 over the pH range that was used (pH 5.5−9.0). The pH of the reaction was measured before and after the experiment. To prevent the oxidation of catechins, the reaction mixture contained 1 mM ascorbic acid. Assays were started by the addition of enzyme. In the absence of the enzyme, the rate of absorbance change was negligible. Although the DHFR-catalyzed reaction has been shown to occur via a random mechanism (*18*), it can be simplified to an ordered mechanism whenever [NADPH] ≫ [DHF] (i.e., A ≫ B). The values of the maximum steady-state rate (V_{max})[2] and the Michaelis constant of DHFR for DHF (K_m^B) were determined from the curvature evident in plots of the disappearance of NADPH and DHF versus time (10 determinations). For K_m^B determinations, the initial concentration of saturating NADPH (100 μM) was considered to be constant during the consumption of 10 μM DHF by the enzyme (6 nM). Data were fitted by nonlinear regression to the integrated form (*19*) of the Michaelis equation, using Marquart's algorithm (*20*) implemented in Sigma Plot 2.01 for Windows (*21*). When NADPH is the first substrate to bind to the enzyme, its Michaelis constant ($K_m^A = k_5/k_1$) cannot be directly determined from this experimental procedure. K_m^A was indirectly calculated from k_{cat} (k_5) and k_1 values obtained from separate experiments.

Fluorescence Studies. The fluorescence of DHFR is reduced upon binding of substrates and inhibitors, and this property may be used as a convenient method for determining both the enzyme concentration and the dissociation constants of enzyme−ligand complexes. Dissociation constants for the binding of NADPH (K_d^A) and inhibitors (EGCG or ECG) (K_I^E) to free DHFR were determined by fluorescence titration in an automatic scanning Perkin-Elmer LS50B spectrofluorimeter with 1.0 cm light path cells equipped with a 150 W xenon (XBO) light source. The formation of the binary complex between the enzyme and the ligand was followed by assessing the quenching of tryptophan fluorescence of the enzyme upon addition of microliter volumes of a concentrated stock solution of ligand. Fluorescence emission spectra were recorded when DHFR fluorescence was excited at 290 nm. Dissociation constants of the preformed E−NADPH complex (made by addition of 0.1 mM NADPH to 0.25 μM enzyme) with inhibitors (K_I^{EA}) were determined by fluorescence quenching titration at 440 nm (excited at 340 nm). All measurements were corrected for dilution, and the data from the titration curves were fitted as described previously (*17*). Titrations were performed in the same buffers as described for DHFR assays. The temperature was controlled at 25 °C using a Haake D1G circulating bath with a heater and cooler. Stopped-flow fluorescence experiments were carried out using an Applied Photophysics Ltd. (Leatherhead, U.K.) Pi-Star 180 spectrometer (75 W Xe light source) with a stopped-flow unit at 25 °C (Neslab RTE-7 circulating bath). The apparatus was operated in single-mixing mode using the 2 mm path length observation cell and demonstrated a dead time of approximately 1.1 ms. The reaction of bovine liver DHFR (0.25 μM) with NADPH or inhibitors was observed under pseudo-first-order conditions by fluorescence at 340 nm (excitation at 290 nm). Concentrations of the reagents are given in the Results and figures. The kinetic data were fitted to exponential functions using the Pi-Star 180's nonlinear regression curve fitting program. The data points shown in the figures are the means of at least three (normally five) repeat observations.

Spectrophotometric Assays. Ultraviolet−visible absorption spectra of catechins at different pHs were recorded on a UV−vis Perkin-Elmer Lambda-2 spectrophotometer with a spectral bandwidth of 1 nm at a scan speed of 60 nm s^{-1}. The assay medium was like that used for kinetic assays. Reference cuvettes contained all the components except the inhibitor in a final volume of 1 mL.

Dihydrofolate Reductase Inhibition Experiments. The slow development of catechin inhibition was assessed by continuously monitoring the disappearance of NADPH and DHF after initiation of the reaction by the addition of DHFR (3.3 nM). Reaction mixtures contained buffer, NADPH, DHF, and various concentrations of EGCG or ECG. Progress curves were obtained under ordered conditions ([NADPH] ≫ [DHF]). Experiments to determine the recovery of enzyme activity after inhibition by preincubation with catechins were performed as follows. DHFR (165 nM) was preincubated for 70 min at 25 °C in the buffer mixture containing catechin (40 μM) and ascorbic acid (1 mM) in the absence or presence of different concentrations of NADPH. Aliquots (20 μL) of the incubation mixture was then diluted 50-fold into a reaction mixture containing the buffer mixture, NADPH (100 μM), and DHF (10 μM) to give a final enzyme concentration of 3.3 nM. Reaction mixtures contained 0.8 μM catechin, following dilution from the incubation mixtures. Recovery of enzyme activity was followed by continuous monitoring at 340 nm.

Kinetic Simulations. Kinetic simulation experiments have been designed to distinguish between parts A and B of Scheme 2 (Table 2) and Scheme 3 (Table 3). The kinetics of the reaction mechanisms described in these schemes are defined by a set of differential equations, whose numerical integrations were carried out with a computer program designed by García-Sevilla et al. (*22*). Experimentally determined values of the equilibrium and rate constants were assigned to the partial reactions defined in these schemes. Preincubation of the enzyme (E) with an excess of EGCG (I) with and without NADPH (A) generates an equilibrium between the enzymatic species present in the samples, which will vary depending on the action mechanism (E, E−A, E−I, and E*−I for Scheme 2A; E, E−A, E−A−I, and E*−A−I for Scheme 2B; and E, E−A, E−I, and E−A−I for Scheme 3). In simulated experiments, the concentrations of the enzyme species at different NADPH concentrations, after reaction for 70 min, were calculated by numerical integration of the schemes in the absence of catalysis (without addition of species B), using the dissociation constants presented in Tables 4 and 5. Recovery of enzyme activity by one of these two mechanisms can be simulated (with addition of species A and B) using the initial concentrations for the enzymatic species calculated as described above and the remaining inhibitor concentration carried over with the preincubated enzyme (0.8 μM).

RESULTS

Inhibition of Bovine Liver Dihydrofolate Reductase by Tea Catechins. Green tea extracts containing significant amounts of tea catechins strongly inhibited the activity of bovine liver

[2] Notation and definitions: E, free DHFR; A, NADPH; B, DHF; P, $NADP^+$; Q, THF; I, EGCG or ECG; EGCGH, protonated species of EGCG; $EGCG^-$, deprotonated species of EGCG; V_{max}, maximum steady-state rate ($V_{max} = k_{cat}[E]$); k_{cat}, catalytic constant ($k_{cat} = k_5$); v_0, velocity of the first steady state; v_s, velocity of the final steady state; k_{obs}, apparent first-order inhibition rate constant; k_{obs}^{max}, maximum apparent first-order inhibition rate constant at a saturating inhibitor concentration; k_{app}, pseudo-first-order rate constant for the binding of I to E; k_x ($x = 1-11$), rate constants of the reaction mechanism of DHFR; K_d^A, dissociation constants of E toward *A* ($K_d^A = k_2/k_1$); K_m^A and K_m^B, Michaelis constants of DHFR toward A and B, respectively [$K_m^A = k_5/k_1$, $K_m^B = (k_4 + k_5)/k_3$]; K_I^E, apparent dissociation constant of E toward I at a particular pH value ($K_I^E = k_7/k_6$); K_I^{EA}, apparent dissociation constant of the complex EA toward I at a particular pH value ($K_I^{EA} = k_9/k_8$); k_{10}^f, first-order rate constant for the formation of a slowly dissociating inhibitor complex; k_{10}^s, second-order rate constant for the reaction of the EI complex with A; K_I^*, inhibition constant for the overall inhibition process {$K_I^* = [k_{11}/(k_{10}^f + k_{11})]K_I^E$ or $K_I^* = [k_{11}/(k_{10}^s[A] + k_{11})]K_I^E$}; K_I^{**}, inhibition constant for the overall inhibition process {$K_I^{**} = [k_{11}/(k_{10}^f + k_{11})]K_I^{EA}$}; K_E, dissociation constant of the deprotonation−protonation equilibrium between EH and E; K_{EA}, dissociation constant of the deprotonation−protonation equilibrium between EAH and EA; K_C, dissociation constant of the deprotonation−protonation equilibrium between EGCGH and $EGCG^-$; K_I^{EGCGH}, pH-independent dissociation constant for the E−EGCGH complex; $K_I^{EGCG^-}$, pH-independent dissociation constant for the E−$EGCG^-$ complex.

Table 1: Possible Mechanisms for the Slow-Binding Inhibition of DHFR Assuming an Initial Slow-Binding Process and Their Relationship to the Apparent First-Order Constant (k_{obs}) and Steady-State Rates v_0 and v_s[a]

mechanism	k_{obs}	*steady-state rates*
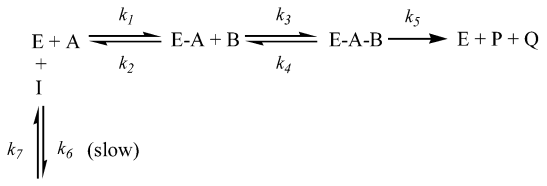 (Scheme 1*A*)	$k_{obs} = k_6\alpha[I] + k_7$ $\alpha = K_d^A K_m^B + K_m^A[B]/\left(K_d^A K_m^B + K_m^B[A] + K_m^A[B] + [A][B]\right)$	$v_0 = \dfrac{V_{max}[A][B]}{K_d^A K_m^B + K_m^B[A] + K_m^A[B] + [A][B]}$ $v_s = \dfrac{V_{max}[A][B]}{K_d^A K_m^B\left(1 + \dfrac{[I]}{K_I^E}\right) + K_m^B[A] + K_m^A\left(1 + \dfrac{[I]}{K_I^E}\right)[B] + [A][B]}$
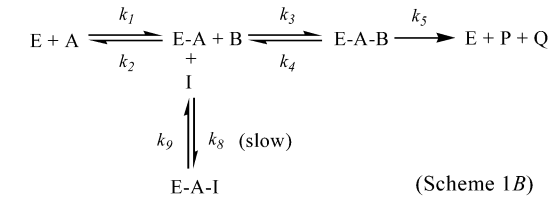 (Scheme 1*B*)	$k_{obs} = k_8\alpha[I] + k_9$ $\alpha = K_m^B[A]/\left(K_d^A K_m^B + K_m^B[A] + K_m^A[B] + [A][B]\right)$	$v_0 = \dfrac{V_{max}[A][B]}{K_d^A K_m^B + K_m^B[A] + K_m^A[B] + [A][B]}$ $v_s = \dfrac{V_{max}[A][B]}{K_d^A K_m^B + K_m^B\left(1 + \dfrac{[I]}{K_I^{EA}}\right)[A] + K_m^A[B] + [A][B]}$

[a] Where $K_d^A = k_2/k_1$, $K_m^A = k_5/k_1$, $K_m^B = (k_4 + k_5)/k_3$, $K_I^E = k_7/k_6$, and $K_I^{EA} = k_9/k_8$.

Table 2: Possible Mechanisms for the Slow-Binding Inhibition of DHFR Assuming an Isomerization to a Slowly Dissociating Inhibition Complex and Their Relationship to the Apparent First-Order Rate Constant (k_{obs}) and Steady-State Rates v_0 and v_s

mechanism	k_{obs}	*steady-state rates*
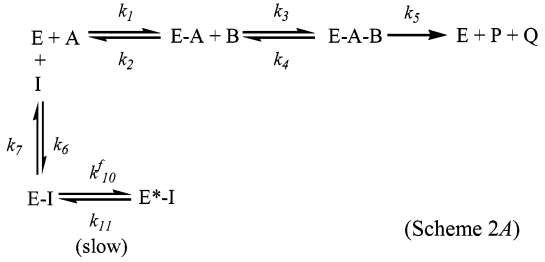 (Scheme 2*A*)	$k_{obs} = \dfrac{\alpha_1 + \alpha_2[I]}{\alpha_3 + [I]}$ $\alpha_1 = k_{11}K_I^E\left(\dfrac{K_d^A K_m^B + K_m^B[A] + K_m^A[B] + [A][B]}{K_d^A K_m^B + K_m^A[B]}\right)$ $\alpha_2 = k_{10}^f + k_{11}$ $\alpha_3 = K_I^E\left(\dfrac{K_d^A K_m^B + K_m^B[A] + K_m^A[B] + [A][B]}{K_d^A K_m^B + K_m^A[B]}\right)$	$v_0 = \dfrac{V_{max}[A][B]}{K_d^A K_m^B\left(1 + \dfrac{[I]}{K_I^E}\right) + K_m^B[A] + K_m^A\left(1 + \dfrac{[I]}{K_I^E}\right)[B] + [A][B]}$ $v_s = \dfrac{V_{max}[A][B]}{K_d^A K_m^B\left(1 + \dfrac{[I]}{K_I^*}\right) + K_m^B[A] + K_m^A\left(1 + \dfrac{[I]}{K_I^*}\right)[B] + [A][B]}$
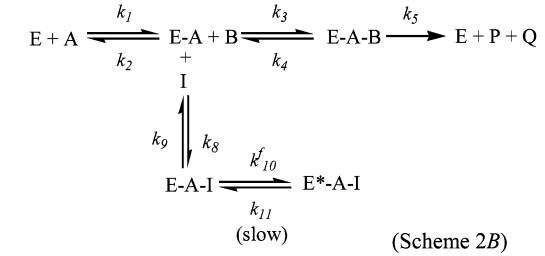 (Scheme 2*B*)	$k_{obs} = \dfrac{\alpha_1 + \alpha_2[I]}{\alpha_3 + [I]}$ $\alpha_1 = k_{11}K_I^{EA}\left(\dfrac{K_d^A K_m^B + K_m^B[A] + K_m^A[B] + [A][B]}{K_d^B K_m^A + K_m^B[A]}\right)$ $\alpha_2 = k_{10}^f + k_{11}$ $\alpha_3 = K_I^{EA}\left(\dfrac{K_d^A K_m^A + K_m^B[A] + K_m^A[B] + [A][B]}{K_m^B[A]}\right)$	$v_0 = \dfrac{V_{max}[A][B]}{K_d^A K_m^B + K_m^B\left(1 + \dfrac{[I]}{K_I^{EA}}\right)[A] + K_m^A[B] + [A][B]}$ $v_s = \dfrac{V_{max}[A][B]}{K_d^A K_m^B + K_m^B\left(1 + \dfrac{[I]}{K_I^{**}}\right)[A] + K_m^A[B] + [A][B]}$

Table 3: Possible Mechanism for the Slow-Binding Inhibition of DHFR Assuming the Formation of a Slowly Dissociating Complex after the Reaction of NADPH with the Enzyme−Inhibitor Complex and Their Relationship to the Apparent First-Order Rate Constant (k_{obs}) and Steady-State Rates v_0 and v_s

mechanism	k_{obs}	*steady-state rates*
$E + A \underset{k_2}{\overset{k_1}{\rightleftharpoons}} E\text{-}A + B \underset{k_4}{\overset{k_3}{\rightleftharpoons}} E\text{-}A\text{-}B \xrightarrow{k_5} E + P + Q$ $+$ $I \underset{k_7}{\overset{k_6}{\rightleftharpoons}} E\text{-}I + A \underset{k_{11}\ \text{(slow)}}{\overset{k'_{10}}{\rightleftharpoons}} E\text{-}A\text{-}I$ (Scheme 3)	$k_{obs} = \dfrac{\alpha_1 + \alpha_2[I]}{\alpha_3 + [I]}$ $\alpha_1 = k_{11}K_I^E\left(\dfrac{K_d^A K_m^B + K_m^B[A] + K_m^A[B] + [A][B]}{K_d^A K_m^B + K_m^A[B]}\right)$ $\alpha_2 = k'_{10}[A] + k_{11}$ $\alpha_3 = K_I^E\left(\dfrac{K_d^A K_m^B + K_m^B[A] + K_m^A[B] + [A][B]}{K_d^A K_m^B + K_m^A[B]}\right)$	$v_0 = \dfrac{V_{max}[A][B]}{K_d^A K_m^B\left(1 + \dfrac{[I]}{K_I^E}\right) + K_m^B[A] + K_m^A\left(1 + \dfrac{[I]}{K_I^E}\right)[B] + [A][B]}$ $v_s = \dfrac{V_{max}[A][B]}{K_d^A K_m^B\left(1 + \dfrac{[I]}{K_I^*}\right) + K_m^B[A] + K_m^A\left(1 + \dfrac{[I]}{K_I^*}\right)[B] + [A][B]}$

Table 4: Kinetic Constants for the Reaction of Bovine Liver DHFR with NADPH and DHF at 25 °C and pH 7.6

constant	technique	value
K_d^A (μM)	fluorescence quenching	4.8 ± 0.4
K_m^A (μM)	calculated[a]	1.5 ± 0.2
K_m^B (μM)	integrated Michaelis equation	0.43 ± 0.03
k_{cat} (s^{-1})	integrated Michaelis equation	5.1 ± 1.1
k_1 ($M^{-1}\,s^{-1}$)	transient phase kinetics	$(3.4 \pm 0.3) \times 10^6$
k_2 (s^{-1})	calculated[a]	16.3 ± 2.8

[a] Where $K_m^A = k_{cat}/k_1$ and $k_2 = K_d^A k_1$.

DHFR (Figure 2A). To detect which components of these extracts were responsible for such inhibition, we assayed DHFR activity in the presence of EC, EGC, ECG, or EGCG (Figure 2A). The results showed that both ECG and EGCG were potent inhibitors of the bovine enzyme; however, polyphenols lacking the ester-bonded gallate moiety (e.g., EGC and EC) did not inhibit DHFR. These results indicate that the ester-bonded gallate moiety is essential for inhibition of bovine liver DHFR. When DHFR activity was continuously assayed after addition of enzyme to assay mixtures containing ECG or EGCG and enzyme substrates (NADPH and DHF), the resulting progress curves displayed time-dependent decreases in the reaction rates and finally attained steady-state velocities which varied as a function of inhibitor concentration (Figure 2B,C), suggesting the slow establishment of a steady state between the enzyme, inhibitor, and enzyme−inhibitor complex (*23*). This slow-binding inhibition has previously been reported for the inhibition of DHFR from several biological sources with folate analogues such as MTX and deazafolates (*23*, *24*). Provided that the concentration of free inhibitor is not substantially altered by the formation of any enzyme−inhibitor complex, the progress curve for such inhibition can be described by eq 1:

$$P = v_s t + (v_0 - v_s)[1 - \exp(-k_{obs}t)]/k_{obs} \qquad (1)$$

where v_0, v_s, and k_{obs} represent the initial steady-state velocity, the final steady-state velocity, and the apparent first-order inhibition rate constant, respectively. Plots of k_{obs} against inhibitor (EGCG or ECG) concentration (Figure 3) gave hyperbolic dependencies.

Binding of EGCG and ECG to the Enzyme. The binding of EGCG or ECG to free DHFR was assessed by following the decrease in enzyme fluorescence that occurs upon formation of the enzyme−inhibitor complex. When bovine liver DHFR fluorescence is excited at 290 nm, its emission spectrum shows a maximum at 340−350 nm. The binding of EGCG or ECG quenches this fluorescence (Figure 4A,B). The data for the resulting titration curves were used for K_I^E determinations (Table 5). The data showed that dissociation constants of free DHFR for EGCG (120 nM) and ECG (82 nM) were lower than those for NADPH (4.8 μM) (Tables 4 and 5). The binding of the inhibitors to the free enzyme was investigated at pH 7.6 using stopped-flow fluorescence kinetics. Under pseudo-first-order conditions, the apparent rate of reaction increased linearly with inhibitor concentration and showed no evidence of saturation at higher concentrations (Figure 4C). Assuming a simple association step

$$E + I \underset{k_6}{\overset{k_7}{\rightleftharpoons}} EI$$

Table 5: Kinetic Constants for the Inhibition of Bovine Liver DHFR with Tea Catechins at 25 °C and pH 7.6

constant	technique	I = EGCG	I = ECG
K_I^E (nM)	fluorescence quenching	120 ± 20	82.0 ± 15
	steady-state kinetics	97.6 ± 16	74.3 ± 16
K_I^{EA} (μM)	fluorescence quenching	56.2 ± 8.1	45.4 ± 6.9
k_6 (M^{-1} s^{-1})	transient phase kinetics	$(1.4 \pm 0.2) \times 10^5$	$(1.8 \pm 0.4) \times 10^5$
k_7 (s^{-1})	calculated[a]	$(1.7 \pm 0.5) \times 10^{-2}$	$(1.4 \pm 0.6) \times 10^{-2}$
		$(1.4 \pm 0.4) \times 10^{-2}$	$(1.3 \pm 0.6) \times 10^{-2}$
k_{10}^s (M^{-1} s^{-1})	steady-state kinetics	22.5 ± 2.0	6.3 ± 0.8
k_{11} (s^{-1})	steady-state kinetics[b]	$(1.8 \pm 0.2) \times 10^{-4}$	$(8.8 \pm 1.1) \times 10^{-4}$
K_I^* (nM)	calculated[a]	8.9 ± 3.3	47.8 ± 10
		7.2 ± 2.6	43.1 ± 12

[a] Where $k_7 = K_I^E k_6$ and $K_I^* = [k_{11}/(k_{10}^s[A] + k_{11})]K_I^E$. [b] k_{11} values represent the mean of those calculated from Figures 3 and 5C.

the observed rate (k_{app}) can be approximated by the relationship $k_{app} = k_6[I] + k_7$, where k_6 and k_7 are the rate constants for the association and dissociation, respectively. Thus, a plot of k_{app} against [I] is a straight line with a slope of k_6 and an intercept of k_7 (Figure 4C). Following this scheme, the second-order rate constants for the reaction of DHFR and EGCG or ECG were obtained (Table 5). In each of these experiments, the intercept value of k_7 was too small to be measured; however, it could be calculated from the K_I^E expression ($K_I^E = k_7/k_6$) (Table 5).

To investigate the binding of tea inhibitors to the E−NADPH complex at pH 7.6, the emission spectrum of this complex was recorded when the complex was excited at 350 nm. It has been reported that after addition of MTX or TMP to the E−NADPH complex of *Lactobacillus casei*, DHFR fluorescence was quenched due to the formation of the ternary E−NADPH−I complex (*25*). Addition of EGCG or ECG to the preformed E−NADPH complex produced changes in the fluorescence of this complex (data not shown). The dissociation constants for the binding of inhibitor to the E−NADPH complex (K_I^{EA}) were calculated to be 56.2 and 45.4 μM for EGCG and ECG, respectively, which are approximately 500 times higher than the corresponding dissociation constants for the binding of inhibitors to the free enzyme (K_I^E) (Table 5). Therefore, it can be concluded that the binding of NADPH to the enzyme hindered the subsequent binding of the inhibitors to the binary complex.

Mechanisms for Explaining the Slow-Binding Inhibition of Dihydrofolate Reductase. Although the DHFR-catalyzed reaction has been shown to occur via a random mechanism (*18*, *26*), it can be simplified to an ordered mechanism whenever [NADPH] ≫ [DHF]. Under such conditions and considering that EGCG and ECG are structural analogues of DHF, the possible mechanisms that explain the slow-binding inhibition of bovine liver DHFR are depicted in Tables 1−3. Table 1 includes mechanisms assuming an initial slow-binding process. Recently, we have proposed such a mechanism for the slow-binding inhibition of *Stenotrophomonas maltophilia* DHFR by MTX (*27*). Table 2 shows mechanisms in which an enzyme−inhibitor complex is formed rapidly and then undergoes slow isomerization (conformational change) to a slowly dissociating E*−I complex. Scheme 2B, included in this table, has been used to explain the slow, tight-binding inhibition by MTX of DHFR from different biological sources, including *Streptococcus faecium* A and *Escherichia coli* (*17*, *23*). These authors present kinetic evidence that MTX reacts with the E−NADPH complex and not with the free enzyme. More

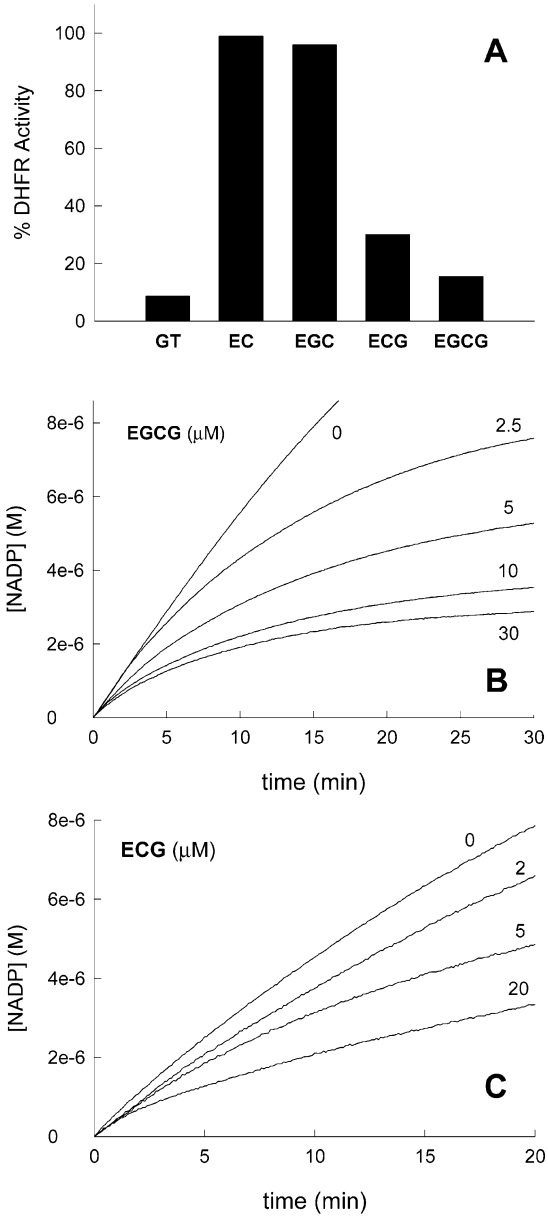

FIGURE 2: Inhibition of bovine liver DHFR activity by tea polyphenols. (A) Relative DHFR inhibition by a green tea extract (GT at 50 μg/mL) and tea catechins (EC, EGC, ECG, and EGCG at 100 μM) with respect to a control experiment with no compound added. Each bar represents the mean of five separate experiments. (B and C) Progress curves for the slow-binding inhibition of bovine liver DHFR by EGCG and ECG, respectively. All the experiments in this figure were carried out at pH 7.6 and 25 °C in the presence of NADPH (100 μM), DHF (10 μM), and DHFR (3.3 nM).

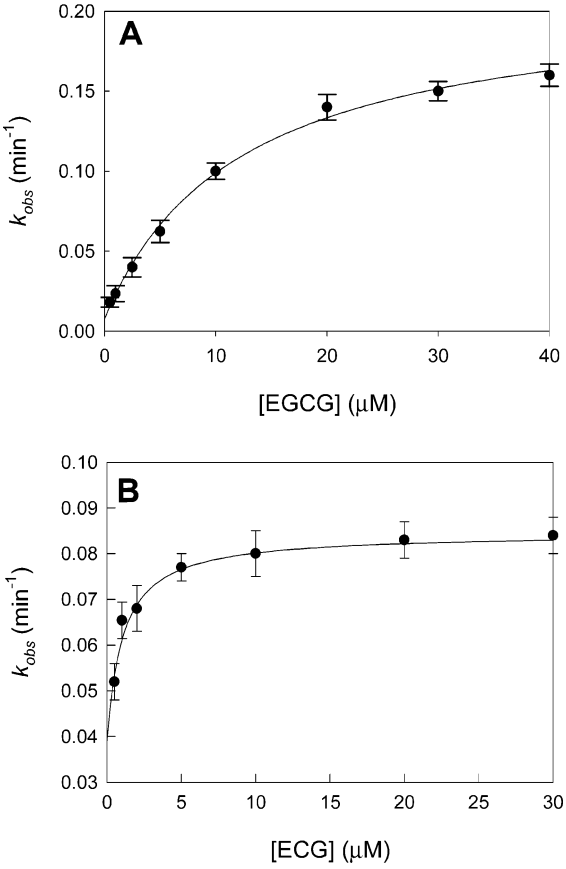

FIGURE 3: Concentration-dependent inhibition of bovine liver DHFR by EGCG (A) or ECG (B). Nonlinear regression analysis of the progress curves presented in panels B and C of Figure 2 to eq 1 yields the values of k_{obs} at different EGCG or ECG concentrations. Results are the mean ± the standard deviation of triplicate determinations.

controversial is the structural reason for this slow isomerization process. Although the interaction of the side chain of MTX with amino acids at the active site of the enzyme, such as Ile-50, Phe-31, and Leu-28, has been proposed as the origin of the slow-binding inhibition, no really convincing evidence for this interaction has been presented. The mechanism described in Table 3 assumes that the origin of the slow-binding inhibition is the formation of a slowly dissociating complex after the reaction of NADPH with the enzyme−inhibitor complex. Although the formation of ternary complexes between DHFR, coenzyme, and inhibitors has been comprehensively demonstrated (*25*, *28*), these mechanisms have not been used to explain the slow-binding inhibition of DHFR, probably due to the high values calculated for the second-order rate constants of the reaction of NADPH with E−MTX and E−TMP complexes. Tables 1−3 also show the analytical expressions for k_{obs}, v_0, and v_s deduced for the proposed mechanisms. In addition to these mechanisms, the origin of this slow-binding behavior could be explained by a model in which the inhibitor binds only (or preferentially) to one of two slowly interconverting conformations of the enzyme, as presented in the context of MTX binding to *E. coli* DHFR (*29*, *30*). A kinetic characteristic of this hysteretic mechanism, when determined by stopped-flow fluorescence quenching, is the presence of a slow inhibitor concentration-independent process due to the slow isomerization of the enzyme (*29*). Stopped-flow experiments carried out in our laboratory for the binding of EGCG or ECG showed time course traces that fit to a single-exponential function which has a linear dependence on inhibitor concentration (Figure 4C). Although hysteretic behavior has been described for bovine liver DHFR, this process should occur over a time scale different from that of the slow-binding inhibition of the enzyme. In fact, Appleman et al. (*4*) compared the hysteretic behavior of DHFR from various sources and reported that human and bovine DHFR exhibited such behavior on a time scale almost 1000 times shorter than that of the bacterial enzymes, i.e., in the 50−150 ms range.

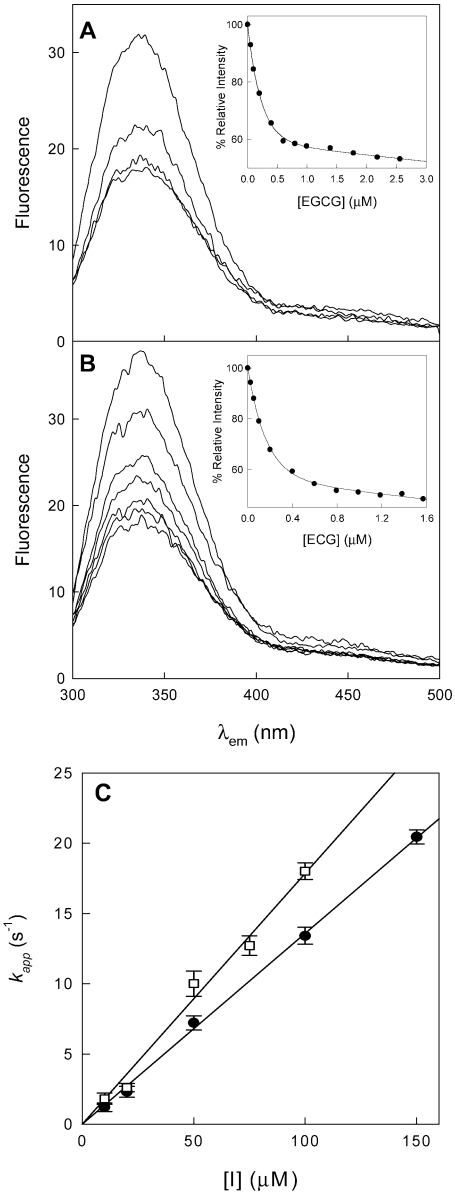

FIGURE 4: Titration and stopped-flow fluorescence experiments for the binding of tea catechins to bovine liver DHFR. Quenching of enzyme fluorescence by the addition of EGCG (A) and ECG (B) (cf. Experimental Procedures). (C) Dependence of the pseudo-first-order rate constant (k_{app}) for the binding of EGCG and ECG to bovine liver DHFR on inhibitor concentration. Stopped-flow fluorescence experiments were carried out at pH 7.6 and 25 °C using an enzyme concentration of 0.25 μM.

Origin of the Slow-Binding Inhibition of Bovine Liver Dihydrofolate Reductase by Tea Catechins. Binding and inhibition experiments were designed to distinguish between

the mechanisms presented in Tables 1−3. Two kinetic features (*31*) are characteristic of an initial slow binding of the inhibitor (mechanisms proposed in Table 1): (i) the initial reaction velocities (v_0) should be independent of inhibitor concentration and (ii) a plot of k_{obs} against the inhibitor concentrations should give a straight line with no saturation kinetics (see expressions for k_{obs} and v_0 in Table 1). The experimental data did not agree with either of these characteristics: it is evident from the progress curves (Figure 2B,C) that the initial activity decreases as a function of inhibitor concentration and saturation kinetics were clearly obtained from a representation of k_{obs} versus inhibitor concentration (Figure 3). Therefore, it can be concluded that the inhibition of DHFR by tea catechins is not due to the formation of a slowly dissociating E−I complex.

The two features described above are not enough to distinguish between the mechanisms listed in Tables 2 and 3, because each predicts variations of v_0 versus the inhibitors and saturation kinetics of k_{obs} versus inhibitor concentration. Inhibition of DHFR by EGCG occurs in the absence of catalysis (preincubation experiments), and the results of enzyme activity recovery in a standard DHFR assay may indicate the type of inhibition. Preincubation of DHFR with EGCG in the absence of NADPH, for 70 min (sufficient time to reach equilibrium), did not produce any observable inhibition in the recovered enzyme activity as compared with a control experiments assayed in the presence of 0.8 μM EGCG (inhibitor concentration carried over from the preincubation experiments with the enzyme aliquot) (Figure 5A, traces a and b). However, preincubation of the enzyme for the same time with EGCG plus NADPH resulted in considerable loss of enzymatic activity (Figure 5A, trace c). The activity reached a value which was ca. 30% of the control activity. Results show that after the addition of preincubated aliquots to the DHFR assay medium there is a readjustment of the concentrations of the enzyme species to rapidly reach the final steady-state rate (v_s). The experimental dependencies of v_s on the concentration of NADPH are shown in Figure 5B. This parameter decreased as the concentration of NADPH increased to a final saturating value. Simulation experiments designed to reproduce these experimental conditions using Schemes 2A, 2B, and 3 show that only Scheme 3 can explain the data. These observed dependencies are the result of the dependence of v_s on NADPH concentration, which is included as part of the K_I^* parameter (Table 3). The results of the experimental and simulated assays presented in Figure 5 demonstrate that the slow-binding inhibition of bovine liver DHFR is due to the formation of a slowly dissociating ternary complex (E−I−NADPH) after the reaction of NADPH with the binary E−I complex (Table 3). Scheme 2A predicts inhibition of DHFR after its incubation in both the absence and presence of NADPH, and therefore, Scheme 2A can be discarded as an inhibition mechanism. Although the mechanism presented in Scheme 2B (Table 2) could represent a possibility for the inhibition of DHFRs isolated from other biological sources with other antifolates, such as MTX (*17*, *23*), several pieces of experimental evidence presented here show that it is not the case for the inhibition of bovine DHFR by tea catechins: (i) simulated experiments of this mechanism did not fulfill the observed dependencies; (ii) the values for the

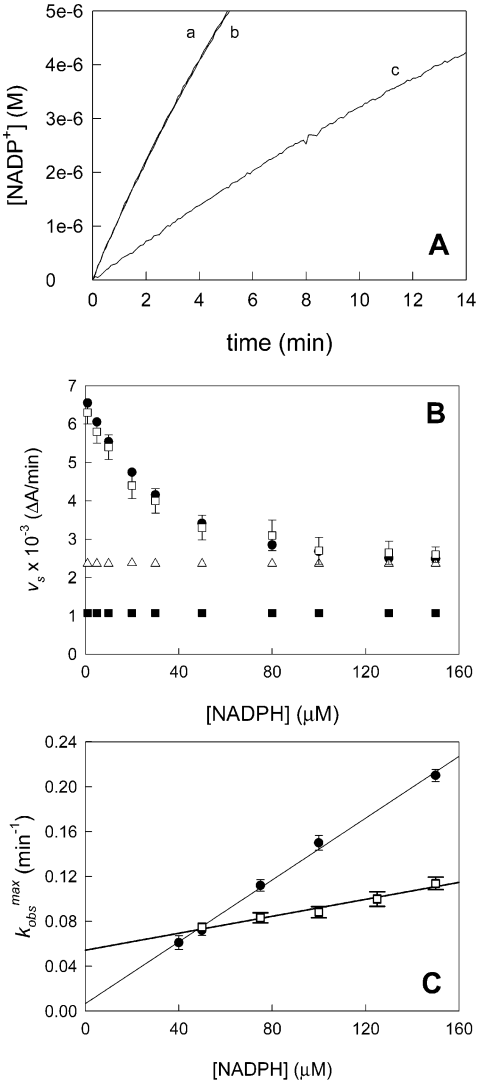

FIGURE 5: Effect of NADPH on the inhibition of bovine liver DHFR by tea catechins. (A) Progress curves for the recovery of the DHFR activity after preincubation for 70 min without EGCG (trace a), with EGCG (40 μM) (trace b), and with EGCG (40 μM) and NADPH (40 μM) (trace c). Assays were initiated by addition to reaction mixtures ([NADPH] = 100 μM and [DHF] = 10 μM at pH 7.6; for trace a, the reaction medium was supplied with 0.8 μM EGCG) of aliquots of the preincubation mixture. (B) Experimental (□) and simulated values of v_s using Scheme 2A (△), 2B (■), or 3 (●). Experimental values were obtained as described in the legend of Figure 6A by DHFR preincubation experiments with EGCG (40 μM) at different NADPH concentrations. For simulated experiments, the concentration distribution of the initial enzyme (3.3 nM) into the different enzymatic species at different NADPH concentrations, after reaction for 70 min, was calculated by numerical integrations of the schemes in the absence of catalysis (without addition of B species). These calculated values were used to initiate the simulation of recovery of activity in the presence of NADPH (100 μM), DHF (10 μM), and EGCG (0.8 μM). The rate constants used for the simulation were as follows: $k_1 = 3.4 \times 10^6$ M^{-1} s^{-1}, $k_2 = 16$ s^{-1}, $k_3 = 1.2 \times 10^7$ M^{-1} s^{-1}, $k_4 = 0.5$ s^{-1}, $k_5 = 5.1$ s^{-1}, $k_6 = k_8 = 1.4 \times 10^5$ M^{-1} s^{-1}, $k_7 = k_9 = 1.7 \times 10^{-2}$ s^{-1}, $k_{10}^f = 2.2 \times 10^{-3}$ s^{-1}, $k_{10}^s = 22$ M^{-1} s^{-1}, and $k_{11} = 1.8 \times 10^{-4}$ s^{-1}. (C) k_{obs}^{max} vs NADPH concentration. Progress curves were obtained at a constant [NADPH]/[DHF] ratio of 5. Nonlinear regression of the progress curves to eq 1 yields the values of k_{obs} at different concentrations of EGCG (●) and ECG (□). Nonlinear regression analysis of curves of k_{obs} vs [EGCG] and [ECG] at different NADPH concentrations to the equation [$k_{obs} = (\alpha_1 + \alpha_2[I])/(\alpha_3 + [I])$] was used for k_{obs}^{max} (α_2 parameter) determinations.

dissociation constants of the inhibitors, calculated from fluorimetric changes at pH 7.6, were ca. 500 times lower for binding to the free enzyme than for the binding to the E−NADPH binary complex (Table 5); and (iii) dissociation constant determinations using steady-state kinetics, EGCG as inhibitor and assuming Scheme 2B, should yield the value of K_I^{EA} (see Table 2). However, such calculations gave a value for the dissociation constant of 71 nM which is closer to the K_I^E value calculated from fluorimetric titrations than to the K_I^{EA} value (Table 5).

Further evidence that favors the mechanism presented in Table 3 versus those described in Table 2 was obtained by representations of k_{obs} versus inhibitor concentration at different concentrations of NADPH. The mechanisms presented in Table 2 predict an independent relationship between k_{obs}^{max} ($k_{obs}^{max} = k_{10}^{f} + k_{11}$) ($\alpha_2$ parameter in Table 2) and NADPH concentration, while the mechanism in Table 3 predicts a linear dependence of k_{obs}^{max} ($k_{obs}^{max} = k_{10}^{s}$[NADPH] + k_{11}) (α_2 parameter in Table 3) with the concentration of NADPH. The results of the experiment designed to test this dependence are shown in Figure 5C and confirm Scheme 3 as the inhibition mechanism of DHFR by tea catechins.

Kinetic Characterization of the Inhibition of Bovine Liver Dihydrofolate Reductase by Tea Catechins. Observation of the steady-state kinetics of DHFR with its natural substrates, NADPH and DHF, is difficult because of the enzyme's low K_m values. To more accurately determine this parameter, progress curves with excesses of NADPH with respect to DHF were analyzed using the integrated Michaelis equation (Table 4). This analysis permits the calculation of V_{max} (k_{cat}) and K_m^B. However, when NADPH is the first substrate to bind to the enzyme, its Michaelis constant ($K_m^A = k_5/k_1$) cannot be directly determined from this procedure. K_m^A was indirectly calculated from k_{cat} (k_5) and k_1 values obtained from separate experiments. Other kinetic parameters necessary for subsequent calculations are also included in Table 4. Plots of k_{obs} versus the concentration of inhibitor (EGCG or ECG) (Figure 3) were fitted by nonlinear regression to the equations that resulted from resolving Scheme 3 (Table 3). The calculated constants are given in Table 5. The value of k_{obs}^{max} ($k_{obs}^{max} = k_{10}^{s}$[A] + k_{11}) was calculated at different concentrations of NADPH using a fixed concentration ratio of NADPH and DHF ([NADPH]/[DHF] = 5). A plot of k_{obs}^{max} versus [NADPH] (Figure 5*C*) was fitted by linear regression, yielding second-order rate constants of 22.5 and 6.3 M^{-1} s^{-1} for the reaction of the E−EGCG and E−ECG complexes with NADPH, respectively. The values of k_{11} calculated from the *y*-axis intercepts of this representation agree with those calculated from steady-state inhibition experiments (Table 5). As can be seen, the values of K_I^E, obtained from the steady-state kinetics of the mechanism involving no binding of the inhibitors to the E−NADPH complex, were similar to the values calculated in fluorescence quenching experiments. Therefore, it can be concluded that, under the experimental conditions used in these experiments, EGCG and ECG do not bind to the E−NADPH binary complex. The inhibition constants for the overall inhibition process (K_I^*) were also calculated (Table 5).

pH Studies. Recent studies have presented data suggesting that the pH could be important for the biological activity of tea catechins, and more specifically for the bactericidal and antifungal activity of EGCG. This tea compound exhibited stronger activity against *Helicobacter pylori* and *Candida albicans* at neutral rather than acid pH (*9*, *32*). These results led us to study the effect of pH on the inhibition of DHFR by tea catechins. Such an effect could arise from the protonation state of bound inhibitor or be related to residues in the active site of the enzyme. Thus, it has been shown that the protonation state of MTX, TMP, and pyrimethanine modulates the binding of these antifolates to DHFRs from several sources (*33*). The absorption spectrum of EGCG is strongly affected by the pH (Figure 6A). The absorbance maximum at 273 nm undergoes a bathochromic displacement to 322 nm, which is greatest at alkaline pH (pH >9.0). Similar spectroscopic characteristics were observed for the other galloylated catechin, ECG (data not shown). To determine if the spectral changes in EGCG and ECG solutions occurring with pH were due to an irreversible oxidation reaction or to a reversible protonation step, a pH titration experiment was carried out. A slightly alkaline solution of EGCG (pH 8.2) was acidified to pH 6.8 by the addition of dilute HCl, and a change in the spectrum of EGCG was observed (Figure 6B), indicating a reversible protonation reaction. The absorption spectra of the nongalloylated counterparts, EC and EGC, showed no significant changes in the pH range of 6.0−8.0 (data not shown). Therefore, the spectral changes with pH observed in EGCG can be attributed to the ester bond gallate moiety with a p*K* of 7.8. At acidic pH, EGCG is mainly present as the protonated species EGCGH, whereas at pH values near neutrality, it evolves toward the deprotonated species $EGCG^-$, which is stabilized by resonance (Figure 6C). The presence of two pH-dependent species of EGCG with the possibility of different hydrogen bond and/or electrostatic interactions could be of interest for further studies on the many important biological actions described for tea catechins (*34*, *35*).

To determine if the protonation state of EGCG had an important effect on the inhibition of bovine liver DHFR, we carried out a complete kinetic characterization of this inhibition at different pH values. The variation of the apparent dissociation constant (K_I^E) for the E−EGCG complex between pH 5.5 and 9.0, as determined by fluorescence titration, is illustrated in Figure 6D. The K_I^E decreased with an increase in pH to a minimum value of approximately 69 nM. Such behavior can be explained by the presence of two p*K*'s that modulate the binding of EGCG to the enzyme. A basic p*K* ($pK_C = 7.8$) arises from the ester bond gallate moiety of the inhibitor, which has been previously calculated from Figure 6A, while a more acidic p*K* (around 7) could represent the p*K* value of a residue in the active site of the free enzyme (pK_E). Essential active site residue Glu-30 is a possible candidate identified by molecular modeling of the interaction between EGCG and DHFR which shows the possibility of hydrogen bonding between a phenolic OH group and Glu-30 (O···O distance of 2.7 Å) (*15*). The pH data appear to indicate a dramatic effect on the binding of EGCG following disruption of this hydrogen bond. A scheme for the interaction of free DHFR with the two ionization forms of EGCG (EGCGH and $EGCG^-$) is shown in Table 6. This model considers that the enzyme with protonated Glu-30 cannot bind to any ionization form of the inhibitor. Data analysis according to the equations derived from this

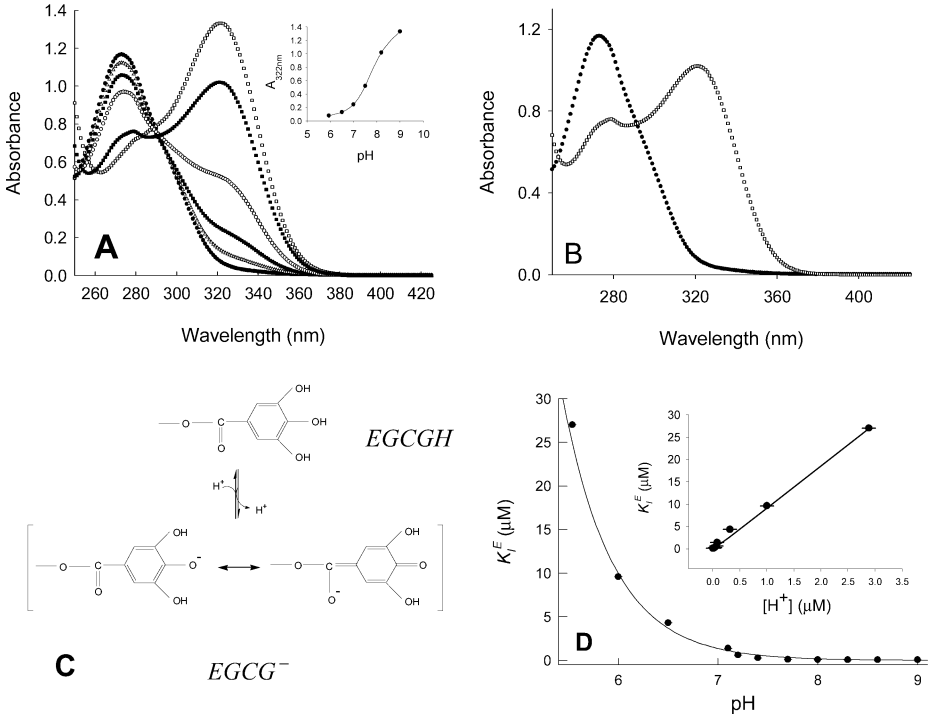

FIGURE 6: Effect of pH on the ionization state of EGCG and on its interaction with bovine liver DHFR. (A) UV−visible absorption spectra of 0.1 mM EGCG at different pH values: (●) 5.9, (△) 6.6, (■) 6.9, (○) 7.5, (▲) 8.0, and (□) 8.9. The inset is a representation of A_{322} vs pH. (B) An EGCG (0.1 mM) solution at pH 8.5 (□) was acidified to pH 6.0 (●) by the addition of dilute HCl. (C) Schematic representation of the effect of pH on EGCG showing the proposed species EGCGH and EGCG⁻. (D) pH dependence of the apparent dissociation constant of bovine liver DHFR for EGCG. The inset shows data points were fitted by nonlinear regression to the equation in Table 6.

Table 6: Mechanism for Explaining the pH Dependencies of the Apparent Inhibition Constant and Its Relationship to Proton Concentration[a]

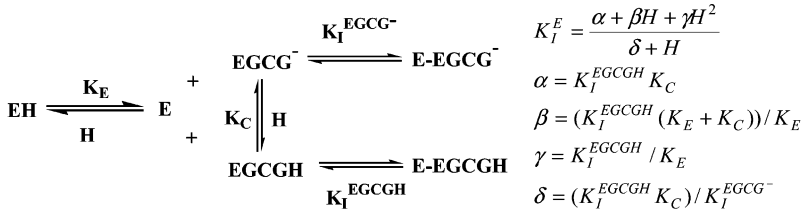

$$K_I^E = \frac{\alpha + \beta H + \gamma H^2}{\delta + H}$$

$$\alpha = K_I^{EGCGH} K_C$$

$$\beta = (K_I^{EGCGH}(K_E + K_C))/K_E$$

$$\gamma = K_I^{EGCGH}/K_E$$

$$\delta = (K_I^{EGCGH} K_C)/K_I^{EGCG^-}$$

Parameter Values for the Variation with pH of the Binding of EGCG to Bovine Liver DHFR			
K_I^{EGCGH} (nM)	$K_I^{EGCG^-}$ (nM)	pK_E	pK_C
605 ± 52	69.9 ± 7.1	6.8 ± 0.1	7.8 ± 0.1

[a] Dissociation constants obtained by fluorescence titration were analyzed according to the equation displayed in this table to yield the parameter values.

mechanism (Table 6) yields values of 6.8 and 7.8 for pK_E and pK_C, respectively. The value of the pH-independent dissociation constant for the protonated and deprotonated forms of the inhibitor (K_I^{EGCGH} and $K_I^{EGCG^-}$, respectively) can also be calculated from this analysis (Table 6). The data suggest that the enzyme in its deprotonated form has a slightly higher affinity for the deprotonated form of the inhibitor. The apparent dissociation constants calculated for the binding of EGCG to the E−NADPH complex (K_I^{EA}) showed different pH dependencies (data not shown). The data suggested a single pK of around pH 7.9, which could be the result of the addition of pK_{EA} and pK_C. The results clearly showed that after the binding of NADPH to the free enzyme there is an increase in the pK of the active site residue responsible for this interaction, possibly Glu-30. Although this is favorable for the reaction of the binary complex with its natural substrate DHF (*36*), the protonation of this protein residue hinders the binding of EGCG to the E−NADPH complex and could explain the high values of K_I^{EA} determined by fluorescence titration at pH 7.6.

DISCUSSION

Antifolate compounds such as MTX are widely used in chemotherapy. Chemotherapeutic agents can elicit a number of cellular responses, including growth arrest and activation of apoptosis or programmed cell death. It has been suggested that apoptosis is an important and ubiquitous mode of death for cells treated with chemotherapeutic drugs. Antifolates

inhibit DHFR, preventing the regeneration of THF, and bringing the folate cycle to a halt. The resulting lack of dTTP causes a nucleotide imbalance, which leads to a misincorporation of nucleotides into the DNA and eventually to the death of the cell by apoptosis. MTX-induced apoptosis in hepatocytes has been recently demonstrated (*37*). Green tea extracts have been shown in vitro to stimulate apoptosis of various cancer cell lines (*7*, *12*−*14*). EGCG has been shown to inhibit several cancer-related proteins (*12*), including urokinase, nitric oxide synthase, telomerase, and tumor necrosis factor α. However, nonphysiological concentrations of EGCG were used in some earlier studies. To determine the molecular targets responsible for the cancer preventive effects of green tea, one must work at concentrations of the molecules that are present physiologically in tea drinkers. Previous studies have indicated that EGCG or other catechins are present in low micromolar concentration ranges (*38*). Therefore, we have shown that gallated tea polyphenols act as DHFR inhibitors in vitro and in vivo (*15*), at concentrations usually found in the blood and tissues of tea drinkers.

DHFR has been isolated and characterized from a wide variety of bacterial and animal sources (*23*, *39*−*41*). These enzymes differ with respect to their type of inhibition by MTX and other folate analogues (*23*, *24*). Thus, both MTX and TMP can be considered as slow tight-binding inhibitors of the enzyme from *E. coli*, but only MTX gives this type of inhibition with the chicken liver enzyme. For the first time, we have demonstrated the direct binding of EGCG and ECG to DHFR, using fluorescence quenching and stopped-flow fluorimetry. These compounds exhibited characteristics of slow-binding inhibitors in bovine enzyme. Experimental data confirm that both compounds are competitive inhibitors with respect to DHF, which bind preferentially to the free enzyme. The origin of their slow-binding inhibition is the formation of a slow dissociation ternary complex by the reaction of NADPH with the E−I complex. Although it is known that MTX can bind efficiently to the free enzyme (*17*) and that NADPH can form a ternary complex by binding to the E−MTX complex (*25*), this kind of mechanism has never been proposed as the origin of the MTX slow tight-binding inhibition of DHFR. Instead, a mechanism in which MTX inhibits by binding to the E−NADPH complex has been suggested (*23*, *25*). The reasons for this proposal are that in the presence of saturating concentrations of NADPH there will be little or no free enzyme with which the inhibitors can interact. However, in the presence of inhibitors, the apparent Michaelis constant for NADPH is K_m^A $(1 + [I]/K_I)$, and therefore, even if the experiments are performed with a 100-fold excess of NADPH over the calculated K_m^A value, the enzyme may be not saturated by this substrate, allowing the entrance of inhibitor to the free enzyme. These results could have important physiological consequences. Although gallated tea polyphenols are structural analogues of DHF, they can compete effectively with the other substrate, NADPH, as a consequence of the random order mechanism. Tumor cells, which grow rapidly, have considerable requirements for both NADPH and DHF. Intracellular depletion of one or both substrates could facilitate the inhibition of DHFR by these tea compounds in tumor cells. Therefore, the inhibition of DHFR by EGCG and ECG could explain, at least in part, its specificity for the growth inhibition of tumor cells.

A comparison of the antifolate activity of EGCG and ECG can be observed in Table 5. Both compounds are potent inhibitors of DHFR at physiological pH. Although ECG can bind slightly better to the free enzyme, this compound is less effective than EGCG due to the fact that ECG can dissociate more rapidly from the ternary inhibitory complex. These data are reflected by the overall inhibition constant K_I^* which is 5 times higher for ECG than for EGCG (Table 5). In any case, the overall inhibition constants of bovine liver DHFR for EGCG and ECG (K_I^*) are in the nanomolar range, and therefore, they are less potent inhibitors of DHFR than MTX, which has a calculated K_I^* in the picomolar range (*23*). The "soft" character of these tea compounds could be developed for use in the prevention and treatment of cancer with significantly reduced side effects compared to those of the DHFR inhibitors currently in use in chemotherapy, such as MTX. The soft character of EGCG together with its ability to induce apoptosis through DHFR inhibition provides a convincing explanation for the epidemiological data on the prophylactic effects of diets high in gallated polyphenols for certain forms of cancer.

Another conclusion drawn from this study is that, in addition to considering the physiological concentration of EGCG, it is also important to consider the pH of the environment in which this catechin acts. The pH controls both the ionization of critical catalytic residues of the enzyme and the protonation state of EGCG and, therefore, the effective concentrations of the protonated and unprotonated forms (Figure 6C). It is expected that each form will exhibit a different affinity and interaction with different molecular target(s) responsible for the cancer preventative effects of EGCG (*34*, *35*). Thus, for DHFR inhibition, the deprotonated form has been proposed to be the more effective inhibitor (Table 6). Arg-70 in human DHFR (a highly conserved residue also found in the bovine liver enzyme) has been shown using X-ray crystallography to interact with the α-carboxylate of the terminal L-glutamate moiety of folic acid or MTX (*3*). Mutation of this residue was found to result in insensitivity to MTX (*42*). Structural modeling of EGCG into human DHFR (*15*) indicates that the compound is oriented in a manner similar to that of MTX or folic acid with the ionizable ester-bonded gallate moiety close to Arg-70 (Figure 1A). The pH-dependent ionization of this gallate could favor formation of a hydrogen bond or electrostatic interaction with Arg-70, thus explaining the higher affinity that we have observed for deprotonated EGCG (Table 6). Additionally, it appears that the ionization state of an essential residue (probably Glu-30) is critical for catechin-dependent inhibition of the bovine enzyme. In fact, when this residue is protonated, EGCG loses its efficiency as an inhibitor of DHFR. EGCG could be defined as a slightly basic inhibitor, and therefore, these pH dependencies could explain why the pH controls the antimicrobial or antifungal action of EGCG against *H. pylori* or *C. albicans*, for which this compound is active at pH 7.0 but not at pH <5.0 (*9*, *32*). This result may condition possible treatments with tea catechins. For example, in the treatment of gastrointestinal diseases associated with *H. pylori*, such as chronic gastritis, peptic ulceration, and gastric cancer, a new, safe, and effective

therapeutic regime against infection could perhaps comprise catechins combined with a proton pump inhibitor (*9*). We are currently examining the possible inhibition of *H. pylori* DHFR by tea catechins. Similarly, the pH could also be important in the effect of EGCG on cancer cells. It has been widely described that the pH inside of cancer cells varies with respect to their normal counterparts. Although there has been a great deal of discussion about whether cancer cells are more acidic or alkaline (*43*), small changes in the intracellular pH could be important for catechin action, and could also be related to the described specificity of these compounds on cancerous versus normal cells.

The data reported in this study clearly demonstrate why antifolates and tea polyphenols have served in similar clinical applications such as antibiotics or in the treatment of cancer and psoriasis (*9*−*11*, *14*, *44*). Moreover, EGCG has considerable potential as a "lead compound" for the development of new anticancer drugs (*16*). The structure of EGCG could be modified to optimize the interaction of the compound with DHFR from a desired biological source or to improve its pharmaceutical properties, for example, to reduce side effects, increase half-life in vivo, reduce the cost of synthesis, improve bioavailability, or increase suitability for a particular method of administration. However, the results also sound a note of caution. Epidemiological studies have linked high levels of green tea consumption by women, around the time of conception and in pregnancy, to an increased incidence of spina bifida and anencephaly (*45*). These are neural tube defects associated with folic acid deficiency. In green tea drinkers, EGCG's antifolate activity would be expected to significantly decrease folic acid levels and minimize the positive effects of folic acid supplements. Thus, this new research provides a possible biochemical explanation for the epidemiological link between heavy green tea drinking and an increased incidence of birth defects.

REFERENCES

1. Lockshin, A., Moran, R. G., and Danenberg, P. V. (1979) Thymidylate synthetase purified to homogeneity from human leukemic cells, *Proc. Natl. Acad. Sci. U.S.A. 76*, 750−754.
2. Blakley, R. L. (1969) *The Biochemistry of Folic Acid and Related Pteridines*, Elsevier, New York.
3. Davies, J. F., II, Delcamp, T. J., Prendergast, N. J., Ashford, V. A., Freisheim, J. H., and Kraut, J. (1990) Crystal structures of recombinant human dihydrofolate reductase complexed with folate and 5-deazafolate, *Biochemistry 29*, 9467−9479.
4. Appleman, J. R., Beard, W. A., Delcamp, T. J., Prendergast, N. J., Freisheim, J. H., and Blakley, R. L. (1989) Atypical transient state kinetics of recombinant human dihydrofolate reductase produced by hysteretic behavior. Comparison with dihydrofolate reductases from other sources, *J. Biol. Chem. 264*, 2625−2633.
5. Lewis, W. S., Cody, V., Galitsky, N., Luft, J. R., Pangborn, W., Chunduru, S. K., Spencer, H. T., Appleman, J. R., and Blakley, R. L. (1995) Methotrexate-resistant variants of human dihydrofolate reductase with substitutions of leucine 22. Kinetics, crystallography, and potential as selectable markers, *J. Biol. Chem. 270*, 5057−5064.
6. Schnell, J. R., Dyson, H. J., and Wright, P. E. (2004) Structure, dynamics, and catalytic function of dihydrofolate reductase, *Annu. Rev. Biophys. Biomol. Struct. 33*, 119−140.
7. Mukhtar, H., and Ahmad, N. (2000) Tea polyphenols: Prevention of cancer and optimizing health, *Am. J. Clin. Nutr. 71*, 1698S−1702S.
8. Fujiki, H., Sugunuma, M., Imai, K., and Nakachi, K. (2002) Green tea: Cancer preventive beverage and/or drug, *Cancer Lett. 188*, 9−13.
9. Mabe, K., Yamada, M., Oguni, I., and Takahashi, T. (1999) In vitro and in vivo activities of tea catechins against *Helicobacter pylori*, *Antimicrob. Agents Chemother. 43*, 1788−1791.
10. Hamilton-Miller, J. M. T. (2001) Anti-cariogenic properties of tea (*Camellia sinensis*), *J. Med. Microbiol. 50*, 299−302.
11. Yam, T. S., Hamilton-Miller, J. M. T., and Shah, S. (1998) The effect of a component of tea (*Camellia sinensis*) on methicillin resistance, PBP2′ synthesis, and β-lactamase production in *Staphylococcus aureus*, *J. Antimicrob. Chemother. 42*, 211−216.
12. Jung, Y. D., and Ellis, L. M. (2001) Inhibition of tumour invasion and angiogenesis by epigallocatechin gallate (EGCG), a major component of green tea, *Int. J. Exp. Pathol. 82*, 309−316.
13. Gupta, S., Hussain, T., and Makhtar, H. (2003) Molecular pathway for (−)-epigallocatechin-3-gallate-induced cell arrest and apoptosis of human prostate carcinoma cells, *Arch. Biochem. Biophys. 410*, 177−185.
14. Yang, G. Y., Liao, J., Kim, K., Yurkow, E. J., and Yang, C. S. (1998) Inhibition of growth and induction of apoptosis in human cancer cell lines by tea polyphenols, *Carcinogenesis 19*, 611−616.
15. Navarro-Perán, E., Cabezas-Herrera, J., García-Cánovas, F., Durrant, M. C., Thorneley, R. N. F., and Rodríguez-López, J. N. (2005) The antifolate activity of tea catechins, *Cancer Res. 65*, 2059−2064.
16. Navarro-Perán, E., Cabezas-Herrera, J., and Rodríguez-López, J. N. (2004) GB Patent 0419181.3.
17. Williams, J. W., Morrison, J. F., and Duggleby, R. G. (1979) Methotrexate, a high-affinity pseudosubstrate of dihydrofolate reductase, *Biochemistry 18*, 2567−2573.
18. Stone, S. R., and Morrison, J. F. (1982) Kinetic mechanism of the reaction catalyzed by dihydrofolate reductase from *Escherichia coli*, *Biochemistry 21*, 3757−3765.
19. Cornish-Bowden, A. (1979) in *Fundamentals of Enzyme Kinetics*, pp 34−37, Butterworth and Co., London.
20. Marquardt, D. W. (1963) An algorithm for least-squares estimation of nonlinear parameters, *J. Soc. Ind. Appl. Math. 11*, 431−441.
21. Jandel Scientific (1994) *Sigma Plot 2.01 for Windows*, Jandel Scientific, Corte Madera, CA.
22. García-Sevilla, F., Garrido del Solo, C., Duggleby, R. G., García-Cánovas, F., Peyro-García, R., and Varón, R. (2000) Use of a windows program for simulation of the progress curves of reactants and intermediates involved in enzyme-catalyzed reactions, *BioSystems 54*, 151−164.
23. Stone, S. R., and Morrison, J. F. (1986) Mechanism of inhibition of dihydrofolate reductases from bacterial and vertebrate sources by various classes of folate analogues, *Biochim. Biophys. Acta 869*, 275−285.
24. Williams, E. A., and Morrison, J. F. (1992) Human dihydrofolate reductase: Reduction of alternative substrates, pH effects, and inhibition by deazafolates, *Biochemistry 31*, 6801−6811.
25. Dunn, S. M. J., and King, R. W. (1980) Kinetics of ternary complex formation between dihydrofolate reductase, coenzyme, and inhibitors, *Biochemistry 19*, 766−773.
26. Andrews, J., Fierke, C. A., Birdsall, B., Ostler, G., Feeney, J., Roberts, G. C. K., and Benkovic, S. J. (1989) A kinetic study of wild-type and mutant dihydrofolate reductases from *Lactobacillus casei*, *Biochemistry 28*, 5743−5750.
27. Navarro-Martínez, M. D., Navarro-Perán, E., Cabezas-Herrera, J., Ruiz-Gómez, J., García-Cánovas, F., and Rodríguez-López, J. N. (2005) Antifolate activity of epigallocatechin gallate against *Stenotrophomonas maltophilia*. *Antimicrob. Agents Chemother*. (in press).
28. Birdsall, B., Burgen, A. S. V., and Roberts, G. C. K. (1980) Binding of coenzyme analogues to *Lactobacillus casei* dihydrofolate reductase: Binary and ternary complexes, *Biochemistry 19*, 3723−3731.
29. Cayley, P. J., Dunn, S. M. J., and King, R. W. (1981) Kinetics of substrate, coenzyme, and inhibitor binding to *Escherichia coli* dihydrofolate reductase, *Biochemistry 20*, 874−879.
30. Rajagopalan, P. T. R., Zhang, Z., McCourt, L., Dwyer, M., Benkovic, S. J., and Hammes, G. G. (2002) Interaction of dihydrofolate reductase with methotrexate: Ensemble and single-molecule kinetics, *Proc. Natl. Acad. Sci. U.S.A. 99*, 13481−13486.
31. Golicnik, M., and Stojan, J. (2004) Slow-binding inhibition: A theoretical and practical course for students, *Biochem. Mol. Biol. Educ. 32*, 228−235.
32. Hirasawa, M., and Takada, K. (2004) Multiple effects of green tea catechin on the antifungal activity of antimycotics against *Candida albicans*, *J. Antimicrob. Chemother*. *53*, 225−229.

33. Cocco, L., Roth, B., Temple, C., Montgomery, J. A., London, R. E., and Blakley, R. L. (1983) Protonated state of methotrexate, trimethoprim, and pyrimethamine bound to dihydrofolate reductase, *Arch. Biochem. Biophys. 226*, 567−577.
34. Nam, S., Smith, D. M., and Dou, Q. P. (2001) Ester bond-containing tea polyphenols potently inhibit proteasome activity *in vitro* and *in vivo*, *J. Biol. Chem. 276*, 13322−13330.
35. Fang, M. Z., Wang, Y., Ai, N., Hou, Z., Sun, Y., Lu, H., Welsh, W., and Yang C. S. (2003) Tea polyphenol (−)-epigallocatechin-3-gallate inhibits DNA methyltransferase and reactivates methylation-silenced genes in cancer cell lines, *Cancer Res. 63*, 7563−7570.
36. Stone, S. R., and Morrison, J. F. (1983) The pH dependence of the binding of dihydrofolate and substrate analogues to dihydrofolate reductase from *Escherichia coli*, *Biochim. Biophys. Acta 745*, 247−258.
37. Kobayashi, K., Terada, C., and Tsukamoto, I. (2002) Methotrexate-induced apoptosis in hepatocytes after partial hepatectomy, *Eur. J. Pharmacol. 438*, 19−24.
38. Yang, C. S. (1997) Inhibition of carcinogenesis by tea, *Nature 389*, 134−135.
39. McTigue, M. A., Davies, J. F., Kaufman, B. T., and Kraut, J. (1992) Crystal structure of chicken liver dihydrofolate reductase complexed with $NADP^+$ and biopterin, *Biochemistry 31*, 7264−7273.
40. Schweitzer, B. J., Srimatkandada, S., Gritsman, H., Sheridan, R., Venkataraghavan, R., and Bertino, J. R. (1989) Probing the role of two hydrophobic active site residues in the human dihydrofolate reductase by site-directed mutagenesis, *J. Biol. Chem. 264*, 20786−20795.
41. Rowe, P. B., and Russel, P. J. (1973) Dihydrofolate reductase. Studies on the activation of the bovine liver enzyme, *J. Biol. Chem. 248*, 984−991.
42. Thompson, P. D., and Freisheim, J. H. (1991) Conversion of arginine to lysine at position 70 of human dihydrofolate reductase: Generation of a methotrexate-insensitive mutant enzyme, *Biochemistry 30*, 8124−8130.
43. Webb, S. D., Sherratt, J. A., and Fish, R. G. (1999) Mathematical modelling of tumour acidity: Regulation of intracellular pH, *J. Theor. Biol. 196*, 237−250.
44. Heydendael, V. M. R., Spuls, P. I., Opmeer, B. C., de Borgie, C. A., Reitsma, J. B., Goldschmidt, W. F., Bossuyt, P. M., Bos, J. D., and de Rie, M. A. (2003) Methotrexate versus cyclosporine in moderate-to-severe chronic plaque psoriasis, *N. Engl. J. Med. 349*, 658−665.
45. Correa, A., Stolley, A., and Liu, Y. (2000) Prenatal tea consumption and risk of anencephaly and spina bifida, *Ann. Epidemiol. 10*, 476−477.

BI050160T